

Bimetallic Photoredox Catalysis: Visible Light-Promoted Aerobic Hydroxylation of Arylboronic Acids with a Dirhodium(II) Catalyst

Hsiang-Ming Yang, Ming-Lun Liu, Jing-Wen Tu, Emily Miura-Stempel, Michael G. Campbell*, and Gary Jing Chuang*



Cite This: *J. Org. Chem.* 2020, 85, 2040–2047



Read Online

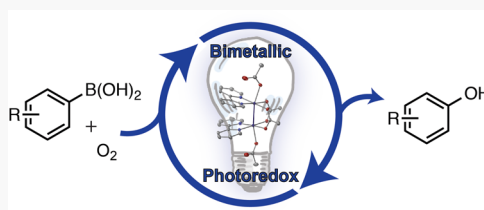
ACCESS |

Metrics & More

Article Recommendations

Supporting Information

ABSTRACT: We report the use of a rhodium(II) dimer in visible light photoredox catalysis for the aerobic oxidation of arylboronic acids to phenols under mild conditions. Spectroscopic and computational studies indicate that the catalyst $\text{Rh}_2(\text{bpy})_2(\text{OAc})_4$ (1) undergoes metal–metal to ligand charge transfer upon visible light irradiation, which is responsible for catalytic activity. Further reactivity studies demonstrate that 1 is a general photoredox catalyst for diverse oxidation reactions.



INTRODUCTION

Photoredox catalysis has been a major focus for organic reaction method development in the past decade.¹ While organic catalysts in photoredox reactions have recently emerged as a promising strategy,² a majority of methods were established based on the archetypal ruthenium(II) catalyst $\text{Ru}(\text{bpy})_3\text{Cl}_2$ and its various derivatives (bpy = 2,2'-bipyridine).³ Among metal-catalyzed photoredox reactions, oxidation reactions that use molecular oxygen provide a mild and environmentally benign route for chemical synthesis.⁴ Such reactions often proceed via generation of the superoxide radical anion in the photoredox cycle.⁵

Dirhodium(II) complexes have long been a privileged class of catalysts and are perhaps the most widely used bimetallic catalysts due to their well-known utility in nitrene and carbene transfer reactions.^{6,7} Only recently, however, rhodium dimers have been studied for electron-transfer reactions in their excited states, an area of research pioneered by the Dunbar and Turro groups.⁸ Inspired by this work, we envisioned that the reactivity of bimetallic rhodium(II) complexes could be expanded to include photoredox catalysis for organic synthesis. Here, we report the first examples of visible light-promoted aerobic oxidation reactions with a dirhodium catalyst. Our work suggests that dirhodium complexes are a promising and highly tunable platform for the development of new photoredox catalysts.

RESULTS AND DISCUSSION

Our investigations began with the visible light-promoted aerobic hydroxylation of arylboronic acids, a transformation originally reported by Jørgenson and Xiao, using $\text{Ru}(\text{bpy})_3\text{Cl}_2$ and subsequently by Scaiano et al. using methylene blue.⁹ As polypyridyl ligands such as bpy are typically key features of photoredox catalysts, with low-lying π^* orbitals that create strong metal-to-ligand charge transfer (MLCT) bands in the

visible region,¹⁰ we targeted the complex $\text{Rh}_2(\text{bpy})_2(\text{OAc})_4$ (1).¹¹ As shown in Table 1, complex 1 is a highly effective catalyst for the aerobic hydroxylation reaction, along with the related 1,10-phenanthroline complex 2. In comparison, dirhodium(II) complexes lacking polypyridyl ligands, such as lactamate complexes 3 and 4, showed substantially reduced photoredox activity; carboxylate complexes $\text{Rh}_2(\text{OAc})_4$ and $\text{Rh}_2(\text{esp})_2$ were completely ineffective catalysts (entries 3–6).¹² Catalyst 1 can be conveniently generated in situ from a mixture of $\text{Rh}_2(\text{OAc})_4$ and bpy (entry 7). The reaction can also proceed in an open flask under air, albeit in a reduced yield as compared to using an O_2 balloon (entry 8). Control experiments clearly establish that both O_2 and light are required for this transformation (entries 9 and 10). When the light source was intermittently turned on and off during the course of the reaction, product generation plateaued during dark periods and resumed when the light was switched back on (Figure 1). This further demonstrates that light is required to sustain catalytic turnover, although we note that the involvement of light-initiated radical chain processes cannot be ruled out.^{13,14}

Exploration of the substrate scope showed that a wide range of arylboronic acids and pinnacol boronic esters can undergo aerobic hydroxylation using catalyst 1, as shown in Table 2. Gram-scale synthesis of 6a was accomplished in 99% isolated yield. Arenes with both electron-donating (alkoxy, 6b–6d) and electron-withdrawing (nitro, 6g,m) substituents gave yields of >80%. Protected and free amino groups were well tolerated (6e,f), along with a range of other substituents including cyano

Received: October 13, 2019

Published: December 30, 2019

Table 1. Reactivity of Rh(II) Dimers in the Hydroxylation of Arylboronic Acids with O₂ and Visible Light

5a	$\xrightarrow[O_2 (1 \text{ atm}), iPr_2NEt (2 \text{ eq.})]{2 \text{ mol \% } [Rh_2] \text{ Catalyst, visible light}^a}$	6a	$\xrightarrow[O_2 (1 \text{ atm}), iPr_2NEt (2 \text{ eq.})]{2 \text{ mol \% } [Rh_2] \text{ Catalyst, visible light}^a}$
Rh ₂ (bpy) ₂ (OAc) ₄ (1)	n = 1, Rh ₂ (pyro) ₄ (3)	n = 3, Rh ₂ (cap) ₄ (4)	
Rh ₂ (phen) ₂ (OAc) ₄ (2)			

^a10.5 W white LED. ^bIsolated yield. ^c2 mol% Rh₂(OAc)₄, 4 mol % bpy, 36 h. ^dn.d. = not detected.

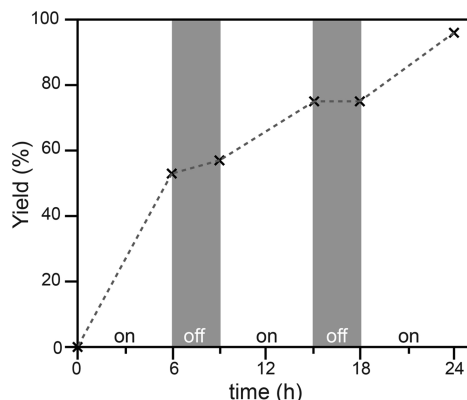


Figure 1. Light source on/off experiment for the conversion of 5a to 6a catalyzed by 1 (conditions as described in Table 1, entry 1), demonstrating that reaction progress pauses and resumes when light is temporarily removed.

groups, esters, acyl groups, and halogens (6h–6s). For the aryl bromide and chloride substrates shown in Table 2, we suspect that the low isolated yields may be due in part to product volatility. Disubstituted (6t–6v), polycyclic (6w–6y), and heterocyclic (6z–6ab) substrates could all be successfully hydroxylated. We were also able to obtain estrone (6ac) via this method in 63% yield from the corresponding pinnacol boronic ester.

Structural characterization of 1 via single crystal X-ray diffraction had not been previously reported, although the structure of the related trifluoroacetate complex was determined.¹¹ We have obtained single crystals of 1 from a DMF solution, confirming the expected structure as shown in Table 1 (Figure S3). Our data suggests that the axial acetate ligands remain coordinated to rhodium in DMF solution: the

Table 2. Aerobic Hydroxylation of Arylboronic Acids with Dirhodium(II) Catalyst 1^a

5	$\xrightarrow[O_2 (1 \text{ atm}), iPr_2NEt (2 \text{ eq.})]{2 \text{ mol \% } 1 \text{ visible light}}$	6
6a, 99% (1.18 g)	6b, R' = Me, 81% 6c, R' = Ph, 97%	6d, 85% 6e, 63%
6f, 74%*	6g, 90% (98%*)	6h, 63% 6i, 46%
6j, R'' = Ph, 99% 6k, R'' = H, 59% (71%*) 6l, R'' = Me, 60%	6m, 95%	6n, 50% 6o, X = Cl, 50% 6p, X = Br, 47% 6q, X = I, 98%
6r, 43%	6s, 20%	6t, 56% 6u, 56%
6v, 73%	6w, 79%	6x, 90% 6y, 74%
6z, 74%	6aa, 69%	6ab, 71% 6ac, 63%*

^aYields reported are for isolated products. Asterisk (*): pinnacol boronic ester (Ar-BPin) used instead of ArB(OH)₂.

structurally related complex [Rh₂(bpy)₂(OAc)₂(MeCN)₂]₂[BF₄]₂ (7)¹¹ in which the axial ligands are replaced with coordinated solvent molecules showed substantially decreased photoredox activity (44% isolated yield for the conversion of 5a to 6a). A comparison of the electronic structures of 1 and 7 shows that replacement of the axial acetate ligands with weaker L-type donors produces significant changes in the energy and relative ordering of the frontier molecular orbitals (Figure S4). Indeed, it is well-established that the ordering of the metal–metal bonding orbitals in dirhodium complexes is highly sensitive to the supporting ligand scaffold.¹⁵ The ability to modulate both the energy and ordering of the Rh–Rh bonding orbitals provides an additional handle for tuning of the electronic structure and reactivity, as compared to mononuclear photoredox catalysts. Studies have shown that weaker axial ligand coordination at rhodium(II) dimers can lead to decreased excited state lifetimes, disfavoring excited state electron transfer processes, which may also account in part for the decreased catalytic activity of 7 compared to 1.^{8b}

As shown in Figure 2a, catalyst 1 dissolved in DMF exhibits two broad absorption bands in the visible spectrum, with $\lambda_{\text{max}} = 445 \text{ nm}$ ($\epsilon = 3900 \text{ M}^{-1} \text{ cm}^{-1}$) and 527 nm ($\epsilon = 1200 \text{ M}^{-1} \text{ cm}^{-1}$). The experimental UV–vis spectrum is well-reproduced

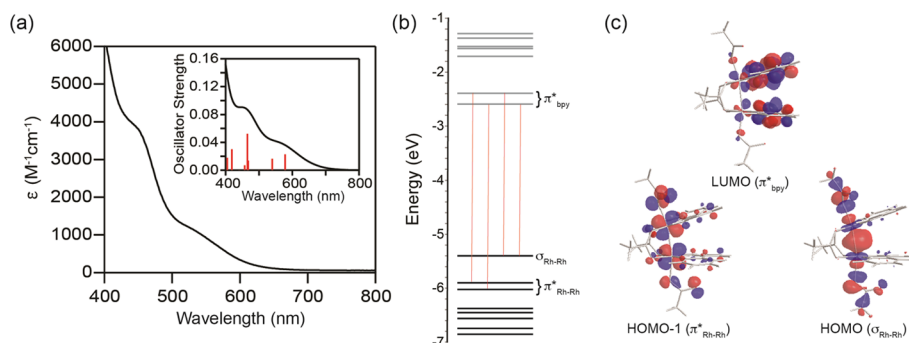


Figure 2. (a) Visible region electronic absorption spectrum of **1** in DMF (the inset shows the TD-DFT calculated spectrum); (b) calculated molecular orbital (MO) diagram for **1**, showing the primary transitions that contribute to visible light absorption; (c) visualizations of selected MOs (details of DFT calculations are given in the Supporting Information).

by time-dependent density functional theory (TD-DFT) calculations on the geometry-optimized structure of **1**. Calculations indicate that both absorption bands in the visible spectrum are due to metal–metal to ligand charge transfer (MMLCT): the lower-energy band arises from $\sigma_{\text{Rh–Rh}} \rightarrow \pi^*_{\text{bpy}}$ transitions, and $\pi^*_{\text{Rh–Rh}} \rightarrow \pi^*_{\text{bpy}}$ transitions produce the higher-energy band (Figure 2b,c). A comparison of LED sources suggests that the higher-energy $\pi^*_{\text{Rh–Rh}} \rightarrow \pi^*_{\text{bpy}}$ MMLCT transitions may be primarily responsible for photocatalytic activity (Table S1). Excitation at 440 nm produces an emission maximum of 468 nm at room temperature for **1** (Figure S5). In combination with the reduction potential measured by cyclic voltammetry (-0.49 V vs SCE; Figure S6), this provides an excited state reduction potential of approximately 2.1 V versus SCE.¹⁶ This potential is more than sufficient to allow for reductive quenching by tertiary amines and is also consistent with the ability to use weaker reductants such as pyridine (Table S2).¹⁷

A plausible mechanism for the observed aerobic hydroxylation reaction with **1** is shown in Figure 3. Following visible

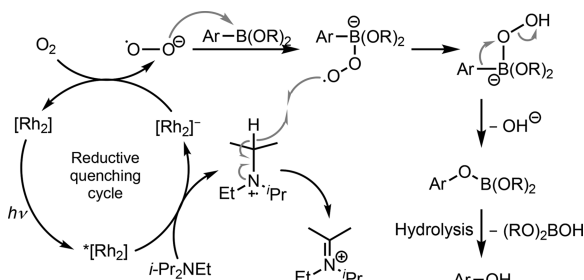


Figure 3. Plausible mechanism for aerobic hydroxylation of arylboronic acids catalyzed by **1**.

light excitation of the catalyst, reductive quenching with Hünig's base would generate an intermediate $[\text{Rh}_2]^-$. Single electron transfer with molecular oxygen would then produce the superoxide radical anion and regenerate the catalyst, and superoxide is capable of arylboronic acid hydroxylation.⁹ Consistent with this mechanism, peroxide generation is observed in the absence of the arylboronic acid substrate but not in the absence of Hünig's base (Table S5), and no product is formed if Hünig's base is omitted from the reaction (Table S1).

To explore the generality of dirhodium(II) complex **1** for photoredox catalysis, we examined several other visible light-promoted oxidation reactions (Figure 4). Aerobic oxidation of

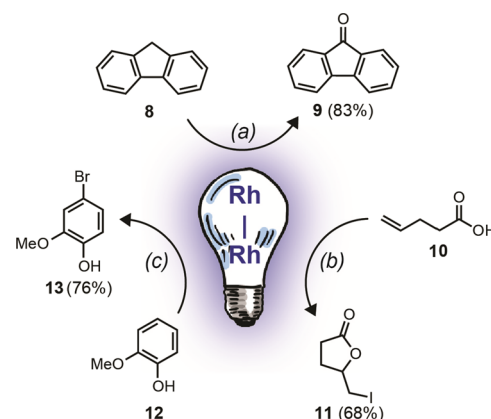


Figure 4. Demonstration of diverse oxidation reactions catalyzed by **1** in the presence of visible light (all reactions conducted with white LED light, room temp., 48 h): (a) 2 mol % **1**, O_2 , DMF, $i\text{-Pr}_2\text{NEt}$; (b) 2 mol % **1**, KI, O_2 , MeOH, AcOH; (c) 5 mol % **1**, CBr_4 , DMF.

activated C–H bonds was found to give fluorenone (**9**) from fluorene (**8**).¹⁸ In situ oxidation of iodide could also promote iodolactonization of **10** to give **11**.¹⁹ Finally, replacement of O_2 with CBr_4 allowed for bromination of guaiacol (**12**) to give **13**.²⁰ We note that these proof-of-concept reactions were conducted without optimization and that negligible background reactions were observed in the absence of either catalyst **1** or light.

In conclusion, we have presented the first use of a rhodium(II) dimer in visible light photoredox catalysis for aerobic oxidation of organic substrates. In addition to cleanly performing hydroxylation of arylboronic acid derivatives, **1** demonstrates reactivity toward a variety of other light-promoted oxidation reactions. We believe that dinuclear rhodium complexes are a promising platform for the development of new photoredox catalysts. In particular, the dirhodium core provides an additional handle for tuning the catalyst's electronic structure and excited state electron transfer reactivity, as compared to more commonly used mononuclear catalysts.

EXPERIMENTAL SECTION

General Information. Reactions were carried out under an ambient atmosphere unless otherwise specified. Methanol and dichloromethane were dried by distillation from CaH_2 . THF, benzene, and toluene were dried by distillation from $\text{Na}/\text{benzophenone}$. Commercially obtained reagents were used as received unless otherwise specified. Visible light photoreactions

were carried out using a 10.5 W white LED strip (180 × Huga 2835 SMD LEDs, luminous flux: 1300 lm) and with continuous stirring. Yields refer to purified and spectroscopically pure compounds. Thin-layer chromatography (TLC) was performed using Merck TLC aluminum sheet silica gel 60 F₂₅₄ plates and visualized by fluorescence quenching under UV light and KMnO₄ stain. Flash chromatography was performed using silica gel (Chromatorex, MB 70-40/75, 40–75 µm) purchased by Fuji Silysia Chemicals. NMR spectra were recorded on a Bruker AVANCE spectrometer operating at 300 MHz for ¹H and 75 MHz for ¹³C and Bruker AVANCE II operating at 400 MHz for ¹H and 100 MHz for ¹³C acquisitions. Chemical shifts are reported in ppm with the solvent resonance as the internal standard. The following solvent chemical shifts were used as reference values (ppm):²¹ CDCl₃ = 7.26 (¹H), 77.16 (¹³C); CD₃OD = 3.31 (¹H), 49.00 (¹³C); DMSO-d₆ = 2.50 (¹H), 39.52 (¹³C). Data is reported as follows: s = singlet, br = broad, d = doublet, t = triplet, q = quartet, m = multiplet; coupling constants in Hz; integration. High-resolution mass spectra were obtained on JMS-700 with a TOF analyzer at the Academia Sinica. Melting points were determined by using a Büchi melting point B-540 melting point apparatus. UV-vis spectra were measured on a Varian Cary 50 spectrophotometer, using quartz cuvettes with a 1 cm path length. Rhodium(II) dimers **1–4**, **7**, and Rh₂(esp)₂ were synthesized according to the previously reported procedures.^{11,12,22–24}

General Procedure for the Aerobic Hydroxylation Reaction in Table 2 (6a as a Representative Example). To a solution of 4-biphenylboronic acid (**5a**, 99 mg, 0.5 mmol) and Rh₂(bpy)₂(OAc)₄ (**1**, 8 mg, 0.01 mmol) in anhydrous DMF (50 mL) in a flame-dried flask was added diisopropylethylamine (170 µL, 1 mmol). The reaction mixture was stirred under an atmosphere of oxygen (1 atm) and visible light irradiation (10.5 W white LEDs). After complete consumption of the starting material (18 h, monitored by TLC), the reaction mixture was poured into ice-cold HCl_(aq) (1%, 50 mL) and extracted with diethyl ether (5 × 50 mL). The combined organic extracts were washed with water (80 mL) and brine (80 mL), dried over MgSO₄, and filtered. After removal of the solvent under vacuum, the crude product was purified by column chromatography (EtOAc/hexanes = 1:8) to give **6a** (81 mg, 95% yield) as a white solid. ¹H NMR (400 MHz, CDCl₃, 21 °C, δ): 7.54 (d, *J* = 7.8 Hz, 2H), 7.48 (d, *J* = 8.1 Hz, 2H), 7.42 (t, *J* = 7.6 Hz, 2H), 7.31 (t, *J* = 7.3 Hz, 1H), 6.91 (d, *J* = 8.2 Hz, 2H), 4.88 (br s, 1H); ¹³C{¹H} NMR (100 MHz, CDCl₃, 22 °C, δ): 155.2, 140.9, 134.1, 128.9, 128.5, 126.9, 115.8; HRMS (EI) *m/z*: [M]⁺ calcd for C₁₂H₁₀O 170.0732; found, 170.0735; FTIR (neat, cm⁻¹) 3415, 3062, 3037, 1944, 1891, 1597, 1523, 1485, 1375, 1243, 1113, 833, 759, 687.

6a from 5a at Gram Scale. To a solution of 4-biphenylboronic acid (**5a**, 1.39 g, 7.0 mmol) and Rh₂(bpy)₂(OAc)₄ (**1**, 112 mg, 0.14 mmol) in anhydrous DMF (700 mL) in a flame-dried flask was added diisopropylethylamine (2.4 mL, 14 mmol). The reaction mixture was stirred under an atmosphere of oxygen (1 atm) and visible light irradiation (21 W white LEDs). After complete consumption of the starting material (36 h, monitored by TLC), the reaction mixture was poured into ice-cold HCl_(aq) (1%, 500 mL) and extracted with diethyl ether (5 × 500 mL). The combined organic extracts were washed with water (500 mL) and brine (500 mL), dried over MgSO₄, and filtered. After removal of the solvent under vacuum, the crude product was purified by column chromatography (EtOAc/hexanes = 1:8) to give **6a** (1.18 g, 99% yield) as a white solid.

6a from 5a Using [Rh₂(Bpy)₂(OAc)₂(MeCN)₂]₂[BF₄]₂ (7) as Catalyst. To a solution of 4-biphenylboronic acid (**5a**, 99 mg, 0.5 mmol) and **7** (9 mg, 0.01 mmol) in anhydrous DMF (50 mL) in a flame-dried flask was added diisopropylethylamine (170 µL, 1 mmol). The reaction mixture was stirred under an atmosphere of oxygen (1 atm) and visible light irradiation (10.5 W white LEDs). After 18 h, the reaction mixture was poured into ice-cold HCl_(aq) (1%, 50 mL) and extracted with ether (5 × 50 mL). The combined organic extracts were washed with water (80 mL) and brine (80 mL), dried over MgSO₄, and filtered. After removal of the solvent under vacuum, the crude product was purified by column chromatography (EtOAc/hexanes = 1:8) to give **6a** (38 mg, 44% yield) as a white solid.

4-Methoxyphenol 6b. Using the general procedure, the crude mixture was purified by column chromatography (EtOAc/hexanes = 1:6) to give the product **6b** (51 mg, 81% yield) as a white solid. ¹H NMR (400 MHz, CDCl₃, 21 °C, δ): 6.83–6.74 (m, 4H), 4.60 (s, 1H), 3.76 (s, 3H); ¹³C{¹H} NMR (100 MHz, CDCl₃, 22 °C, δ): 153.6, 149.6, 116.2, 115.0, 56.0; HRMS (EI) *m/z*: [M]⁺ calcd for C₁₂H₁₀O₂ 186.0681; found, 186.0680; FTIR (neat, cm⁻¹) 3349, 3034, 2924, 2834, 1860, 1607, 1510, 1455, 1375, 1231, 1102, 1031, 824, 734.

4-Phenoxyphenol 6c. Using the general procedure, the crude mixture was purified by column chromatography (EtOAc/hexanes = 1:6) to give the product **6c** (90 mg, 97% yield) as a white solid. ¹H NMR (400 MHz, CDCl₃, 21 °C, δ): 7.36–7.28 (m, 2H), 7.10–7.04 (m, 1H), 7.00–6.92 (m, 4H), 6.87–6.80 (m, 2H), 5.59 (br s, 1H); ¹³C{¹H} NMR (100 MHz, CDCl₃, 22 °C, δ): 158.4, 151.7, 150.2, 129.8, 122.7, 121.1, 117.7, 116.5; HRMS (EI) *m/z*: [M]⁺ calcd for C₁₂H₁₀O₂ 186.0681; found, 186.0680; FTIR (neat, cm⁻¹): 3225, 3026, 1882, 1601, 1587, 1504, 1440, 1342, 1219, 1094, 875, 850, 813, 751, 691.

3-Methoxyphenol 6d. Using the general procedure, the crude mixture was purified by column chromatography (EtOAc/hexanes = 1:10) to give the product **6d** (53 mg, 85% yield) as a pale yellow solid. ¹H NMR (400 MHz, CDCl₃, 24 °C, δ): 7.13 (t, *J* = 8.0 Hz, 1H), 6.51–6.44 (m, 3H), 3.77 (s, 3H); ¹³C{¹H} NMR (100 MHz, CDCl₃, 24 °C, δ): 160.8, 156.8, 130.3, 108.0, 106.4, 101.7, 55.4; HRMS (EI) *m/z*: [M]⁺ calcd for C₇H₈O₂ 124.0524; found, 124.0522; FTIR (neat, cm⁻¹): 3424, 2928, 2854, 1605, 1494, 1462, 1156, 947, 837, 769, 684.

N-(3-Hydroxyphenyl)acetamide 6e. Using the general procedure, the crude mixture was purified by column chromatography (acetone/hexanes = 1:5) to give the product **6e** (47 mg, 63% yield) as a pale yellow solid. ¹H NMR (400 MHz, CD₃OD, 22 °C, δ): 7.16 (s, 1H), 7.10 (t, *J* = 8.10 Hz, 1H), 6.92 (d, *J* = 8.10 Hz, 1H), 6.52 (m, 1H), 2.10 (s, 3H); ¹³C{¹H} NMR (100 MHz, CD₃OD, 22 °C, δ): 171.6, 158.8, 140.9, 130.5, 112.3, 112.1, 23.8; HRMS (EI) *m/z*: [M]⁺ calcd for C₈H₉NO₂ 151.0631; found, 151.0633; FTIR (neat, cm⁻¹): 3330, 3065, 1617, 1568, 1507, 14663, 1377, 1284.

4-Aminophenol 6f. Using the general procedure, the crude mixture was purified by column chromatography (EtOAc/hexanes = 1:5) to give the product **6f** (40 mg, 74% yield) as a dark brown solid. ¹H NMR (400 MHz, CD₃OD, 21 °C, δ): 6.66 (m, 4H); ¹³C{¹H} NMR (100 MHz, CD₃OD, 21 °C, δ): 151.4, 140.1, 118.6, 116.7; HRMS (EI) *m/z*: [M]⁺ calcd for C₆H₇NO 109.0527; found, 109.0527; FTIR (neat, cm⁻¹): 3341, 3281, 3177, 1860, 1615, 1509, 1474, 1386, 1092, 970, 826, 750, 646.

4-Nitrophenol 6g. Using the general procedure, the crude mixture was purified by column chromatography (EtOAc/hexanes = 1:5) to give the product **6g** (64 mg, 91% yield from 4-nitrophenylboronic acid; 68 mg, 98% yield from 4-nitrophenylboronic acid pinacol ester) as a pale yellow solid. ¹H NMR (400 MHz, DMSO-d₆, 21 °C, δ): 11.06 (br s, 1H), 8.08 (d, *J* = 8.9 Hz, 2H), 6.91 (d, *J* = 9.0 Hz, 2H); ¹³C{¹H} NMR (100 MHz, DMSO-d₆, 22 °C, δ): 164.0, 139.7, 126.2, 115.8; HRMS (EI) *m/z*: [M]⁺ calcd for C₆H₅NO₃ 139.0269; found, 139.0271; FTIR (neat, cm⁻¹): 3329, 3120, 3084, 2921, 1589, 1498, 1326, 1287, 1216, 1167, 1113, 851, 755, 629.

4-Hydroxybenzonitrile 6h. Using the general procedure, the crude mixture was purified by column chromatography (EtOAc/hexanes = 1:5) to give the product **6h** (38 mg, 63% yield) as a white solid. ¹H NMR (400 MHz, CDCl₃, 22 °C, δ): 7.56 (d, *J* = 8.00 Hz, 2H), 6.92 (d, *J* = 7.80 Hz, 2H); ¹³C{¹H} NMR (100 MHz, CDCl₃, 21 °C, δ): 159.9, 134.4, 119.3, 116.5, 103.8; HRMS (EI) *m/z*: [M]⁺ calcd for C₇H₅O N 119.0372; found, 119.0371; FTIR (neat, cm⁻¹): 838, 1223, 1449, 1509, 1586, 1612, 2233, 3283.

Methyl 4-Hydroxybenzoate 6i. Using the general procedure, the crude mixture was purified by column chromatography (EtOAc/hexanes = 1:5) to give the product **6i** (35 mg, 46% yield) as a white solid. ¹H NMR (400 MHz, CDCl₃, 24 °C, δ): 7.97 (d, *J* = 8.4 Hz, 2H), 6.87 (d, *J* = 8.5 Hz, 2H), 5.29 (br, 1H), 3.89, (s, 3H); ¹³C{¹H} NMR (100 MHz, CDCl₃, 24 °C, δ): 167.4, 160.2, 132.1, 122.6, 115.4, 52.2; HRMS (EI) *m/z*: [M]⁺ calcd for C₈H₈O₃ 152.0470; found, 152.0473; FTIR (neat, cm⁻¹): 3283, 2233, 1509, 1586, 1166, 838.

4-Hydroxybenzophenone 6j. Using the general procedure, the crude mixture was purified by column chromatography (EtOAc/hexanes = 1:6) to give the product **6j** (98 mg, 99% yield) as a pale yellow solid. ¹H NMR (400 MHz, DMSO-*d*₆, 21 °C, δ): 10.47 (br s, 1H), 7.69–7.63 (m, 4H), 7.60 (t, J = 7.1 Hz, 1H), 7.51 (t, J = 7.7 Hz, 2H), 6.94–6.88 (m, 2H); ¹³C{¹H} NMR (100 MHz, DMSO-*d*₆, 22 °C, δ): 194.4, 126.1, 138.2, 132.6, 131.8, 129.2, 128.4, 128.0, 115.3; HRMS (EI) *m/z*: [M]⁺ calcd for C₁₃H₁₀O₂ 198.0681; found, 198.0676; FTIR (neat, cm⁻¹): 3321, 3055, 1643, 1569, 1510, 1445, 1318, 1283, 1222, 1152, 939, 924, 855, 795, 748, 705, 607.

4-Hydroxybenzaldehyde 6k. Using the general procedure, the crude mixture was purified by column chromatography (EtOAc/hexanes = 1:5) to give the product **6k** (36 mg, 59% yield from boronic acid; 43 mg, 71% yield from boronic acid pinacol ester) as a white solid. ¹H NMR (400 MHz, CDCl₃, 22 °C, δ): 9.88 (s, 1H), 7.82 (d, J = 8.0 Hz, 2H), 6.96 (d, 2H); ¹³C{¹H} NMR (100 MHz, CDCl₃, 25 °C, δ): 191.5, 161.9, 132.6, 129.6, 116.1; HRMS (EI) *m/z*: [M]⁺ calcd for C₇H₆O₂, 122.0369; found, 122.0368; FTIR (neat, cm⁻¹): 3158, 2879, 1905, 1663, 1647, 1588, 1518, 1449, 1385, 1314, 1282, 1215, 1155, 1112, 858, 831, 788.

1-(4-Hydroxyphenyl)ethanone 6l. Using the general procedure, the crude mixture was purified by column chromatography (EtOAc/hexanes = 1:5) to give the product **6l** (41 mg, 60% yield) as a white solid. ¹H NMR (400 MHz, CDCl₃, 22 °C, δ): 7.92 (d, J = 8.6 Hz, 2H), 6.95 (d, J = 8.60 Hz, 2H), 2.85 (s, 3H); ¹³C{¹H} NMR (100 MHz, CDCl₃, 25 °C, δ): 198.5, 161.4, 131.3, 129.8, 115.7, 26.4; HRMS (EI) *m/z*: [M]⁺ calcd for C₈H₈O₂, 136.0520; found, 136.0524; FTIR (neat, cm⁻¹): 3216, 1621, 1580, 1511, 1490, 1460, 1423, 1364, 1257, 1330, 1147, 840.

3-Nitrophenol 6m. Using the general procedure, the crude mixture was purified by column chromatography (EtOAc/hexanes = 1:5) to give the product **6m** (66 mg, 95% yield) as a pale yellow solid. ¹H NMR (400 MHz, DMSO-*d*₆, 21 °C, δ): 10.43 (br s, 1H), 7.60 (d, J = 8.1 Hz, 1H), 7.53 (s, 1H), 7.41 (t, J = 8.1 Hz, 1H), 7.18 (d, J = 8.1 Hz, 1H); ¹³C{¹H} NMR (100 MHz, DMSO-*d*₆, 22 °C, δ): 158.4, 148.8, 130.6, 122.5, 113.9, 109.7; HRMS (EI) *m/z*: [M]⁺ calcd for C₆H₅NO₃, 139.0269; found, 139.0270; FTIR (neat, cm⁻¹): 3379, 3110, 2923, 2853, 1624, 1522, 1350, 1299, 1214, 1078, 998, 934, 876, 818, 739, 672, 605.

Ethyl 2-Hydroxybenzoate 6n. Using the general procedure, the crude mixture was purified by column chromatography (EtOAc/hexanes = 1:5) to give the product **6n** (41 mg, 50% yield) as a yellow oil. ¹H NMR (400 MHz, CDCl₃, 25 °C, δ): 10.58 (s, 1H), 7.86 (d, J = 7.9 Hz, 1H), 7.47 (t, J = 15.6 Hz, 1H), 6.99 (d, J = 8.4 Hz, 1H), 6.90 (t, J = 7.6 Hz, 1H), 4.44 (m, 2H), 1.43 (t, J = 7.1 Hz, 3H); ¹³C{¹H} NMR (75 MHz, CDCl₃, 23 °C, δ): 170.3, 161.7, 135.7, 130.0, 119.2, 117.6, 112.7, 61.5, 14.3; HRMS (EI) *m/z*: [M]⁺ calcd for C₉H₁₀O₃, 166.0626; found, 166.0630; FTIR (neat, cm⁻¹): 3153, 2986, 1675, 1618, 1489, 1375, 1302, 1251, 1213, 1158, 1090, 756, 702, 668.

4-Chlorophenol 6o. Using the general procedure, the crude mixture was purified by column chromatography (ether/pentane = 1:10) to give the product **6o** (33 mg, 50% yield) as a yellow oil. ¹H NMR (400 MHz, CDCl₃, 24 °C, δ): 7.19 (d, J = 8.7 Hz, 2H), 6.77 (d, J = 8.7 Hz, 2H), 5.06 (s, 1H); ¹³C{¹H} NMR (100 MHz, CDCl₃, 24 °C, δ): 154.3, 129.6, 125.6, 116.8; HRMS (EI) *m/z*: [M]⁺ calcd for C₆H₅ClO, 128.0029; found, 128.0032; FTIR (neat, cm⁻¹): 3351, 2928, 1590, 1495, 1433, 1369, 1240, 1095, 822.

4-Bromophenol 6p. Using the general procedure, the crude mixture was purified by column chromatography (EtOAc/hexanes = 1:10) to give the product **6p** (41 mg, 47% yield) as a white solid. ¹H NMR (400 MHz, CDCl₃, 24 °C, δ): 7.35–7.31 (m, 2H), 6.74–6.70 (m, 2H); ¹³C{¹H} NMR (100 MHz, CDCl₃, 24 °C, δ): 154.8, 132.6, 117.3, 112.9; HRMS (EI) *m/z*: [M]⁺ calcd for C₆H₅BrO, 171.9524; found, 171.9528; FTIR (neat, cm⁻¹): 3389, 1587, 1495, 1432, 1236, 1069, 1007, 821 cm⁻¹.

4-Iodophenol 6q. Using the general procedure, the crude mixture was purified by column chromatography (EtOAc/hexanes = 1:9) to give the product **6q** (108 mg, 98% yield) as an orange solid. ¹H NMR (400 MHz, CDCl₃, 24 °C, δ): 7.52 (d, J = 8.7 Hz, 2H), 6.63 (d, J = 8.6

Hz, 2H); ¹³C{¹H} NMR (100 MHz, CDCl₃, 24 °C, δ): 155.2, 138.6, 117.9, 83.0; HRMS (EI) *m/z*: [M]⁺ calcd for C₆H₈O₂ 124.0524; found, 124.0525; FTIR (neat, cm⁻¹): 3386, 2910, 1590, 1496, 1473, 1254, 1206, 830.

3-Chlorophenol 6r. Using the general procedure, the crude mixture was purified by column chromatography (ether/pentane = 1:9) to give the product **6r** (28 mg, 43% yield) as a yellow oil. ¹H NMR (400 MHz, CDCl₃, 24 °C, δ): 7.15 (t, J = 8.1 Hz, 1H), 6.92–6.89 (m, 1H), 6.86 (s, 1H), 6.72 (d, J = 8.0 Hz, 1H); ¹³C{¹H} NMR (100 MHz, CDCl₃, 24 °C, δ): 156.4, 135.0, 130.6, 121.1, 116.0, 113.9; HRMS (EI) *m/z*: [M]⁺ calcd for C₆H₅ClO, 128.0023; found, 128.0029; FTIR (neat, cm⁻¹): 3376, 2927, 2852, 1590, 1475, 1444, 1246, 999, 886, 771, 677.

2-Chlorophenol 6s. Using the general procedure, the crude mixture was purified by column chromatography (ether/pentane = 1:9) to give the product **6s** (13 mg, 20% yield) as a yellow oil. ¹H NMR (400 MHz, CDCl₃, 24 °C, δ): 7.31 (d, J = 8.0 Hz, 1H), 7.54 (t, J = 7.6 Hz, 1H), 7.00 (d, J = 8.0 Hz, 1H), 6.88 (t, J = 15.6 Hz, 1H) 5.60 (s, 1H); ¹³C{¹H} NMR (100 MHz, CDCl₃, 24 °C, δ): 151.7, 129.2, 128.4, 121.3, 120.1, 116.4; HRMS (EI) *m/z*: [M]⁺ calcd for C₆H₅ClO, 128.0030; found, 128.0029; FTIR (neat, cm⁻¹): 3351, 2928, 2854, 1596, 1460, 1751, 1300, 1246, 1035, 845.

2,4-Dimethoxyphenol 6t. Using the general procedure, the crude mixture was purified by column chromatography (EtOAc/hexanes = 1:10) to give the product **6t** (43 mg, 56% yield) as a white solid. ¹H NMR (400 MHz, CDCl₃, 24 °C, δ): 6.83 (d, J = 8.8 Hz, 1H), 6.49 (d, J = 2.4 Hz, 1H), 6.39 (dd, J = 8.8, 2.4 Hz, 1H), 5.23 (s, 1H), 3.86 (s, 3H), 3.76 (s, 3H); ¹³C{¹H} NMR (100 MHz, CDCl₃, 24 °C, δ): 153.5, 147.1, 139.8, 114.2, 104.2, 99.5, 55.9, 55.8; HRMS (EI) *m/z*: [M]⁺ calcd for C₈H₁₀O₃, 124.0524; found, 124.0524; FTIR (neat, cm⁻¹): 3410, 2927, 2851, 1611, 1487, 1478, 1288, 1274, 1189, 1158, 947, 856.

3,5-Dimethoxyphenol 6u. Using the general procedure, the crude mixture was purified by column chromatography (EtOAc/hexanes = 1:10) to give the product **6u** (32 mg, 41% yield) as a white solid. ¹H NMR (400 MHz, CDCl₃, 24 °C, δ): 6.07 (s, 1H), 6.02 (s, 2H), 3.76 (s, 6H); ¹³C{¹H} NMR (100 MHz, CDCl₃, 24 °C, δ): 161.7, 157.5, 94.4, 93.2, 55.4; HRMS (EI) *m/z*: [M]⁺ calcd for C₈H₁₀O₃, 154.0630; found, 154.0631; FTIR (neat, cm⁻¹): 3441, 2924, 2851, 1605, 1460, 1206, 1160, 1063, 823, 679 cm⁻¹.

2,4-Dichlorophenol 6v. Using the general procedure, the crude mixture was purified by column chromatography (EtOAc/hexanes = 1:9) to give the product **6v** (59 mg, 73% yield) as a white solid. ¹H NMR (400 MHz, CDCl₃, 24 °C, δ): 7.33 (d, J = 2.5 Hz, 1H), 7.15 (dd, J = 8.7, 2.4 Hz, 1H), 7.95 (d, J = 16.7 Hz, 1H), 5.56 (s, 1H); ¹³C{¹H} NMR (100 MHz, CDCl₃, 24 °C, δ): 150.3, 128.7, 128.6, 125.7, 120.5, 117.2; HRMS (EI) *m/z*: [M]⁺ calcd for C₆H₄Cl₂O, 161.9639; found, 161.9641; FTIR (neat, cm⁻¹): 3533, 2929, 2853, 2362, 2356, 1650, 1585, 1480, 1410, 1282, 1188, 865, 812, 723.

1-Naphthol 6w. Using the general procedure, the crude mixture was purified by column chromatography (EtOAc/hexanes = 1:8) to give the product **6w** (59 mg, 79% yield) as an orange solid. ¹H NMR (400 MHz, CDCl₃, 21 °C, δ): 8.23–8.15 (m, 1H), 7.86–7.79 (m, 1H), 7.54–7.47 (m, 2H), 7.45 (d, J = 8.3 Hz, 1H), 7.31 (t, J = 7.8 Hz, 1H), 6.82 (d, J = 7.4 Hz, 1H), 5.38 (br s, 1H); ¹³C{¹H} NMR (100 MHz, CDCl₃, 22 °C, δ): 151.5, 134.9, 127.8, 126.6, 126.0, 125.4, 124.5, 121.7, 120.8, 108.7; HRMS (EI) *m/z*: [M]⁺ calcd for C₁₀H₈O, 144.0575; found, 144.0573; FTIR (neat, cm⁻¹): 3257, 3052, 2926, 1699, 1674, 1633, 1598, 1518, 1457, 1386, 1269, 1082, 1043, 1014, 875, 790, 766.

2-Naphthol 6x. Using the general procedure, the crude mixture was purified by column chromatography (EtOAc/hexanes = 1:8) to give the product **6x** (65 mg, 90% yield) as a white solid. ¹H NMR (400 MHz, CDCl₃, 21 °C, δ): 7.77 (t, J = 8.2 Hz, 2H), 7.68 (d, J = 8.2 Hz, 1H), 7.44 (t, J = 7.5, 1H), 7.34 (t, J = 7.5 Hz, 1H), 7.16 (d, J = 2.0 Hz, 1H), 7.12 (dd, J = 8.8, 2.5 Hz, 1H), 5.40 (br s, 1H); ¹³C{¹H} NMR (100 MHz, CDCl₃, 21 °C, δ): 153.5, 134.7, 130.0, 129.0, 127.9, 126.7, 126.5, 123.7, 117.9, 109.6; HRMS (EI) *m/z*: [M]⁺ calcd for C₁₀H₈O 144.0575; found, 144.0576; FTIR (neat, cm⁻¹): 3231,

3050, 2922, 2851, 1630, 1601, 1512, 1467, 1407, 1277, 1216, 959, 844, 814, 741.

2-Methoxy-6-naphthol 6y. Using the general procedure, the crude mixture was purified by column chromatography (EtOAc/hexanes = 1:8) to give the product **6y** (64 mg, 74% yield) as a white solid. ¹H NMR (400 MHz, CDCl₃, 24 °C, δ): 7.65 (d, *J* = 11.6 Hz, 1H), 7.58 (d, *J* = 11.6 Hz, 1H), 7.14–7.05 (m, 4H), 3.90 (s, 1H); ¹³C{¹H} NMR (100 MHz, CDCl₃, 24 °C, δ): 156.2, 151.9, 129.9, 129.8, 128.6, 127.9, 119.4, 118.2, 109.8, 106.1, 55.4; HRMS (EI) *m/z*: [M]⁺ calcd for C₁₁H₁₀O₂, 174.0681; found, 174.0686; FTIR (neat, cm⁻¹): 3307, 2922, 2849, 1624, 1487, 1382, 1379, 1217, 1031, 920, 859, 825, 691.

3,4-Ethylenedioxypheol 6z. Using the general procedure, the crude mixture was purified by column chromatography (EtOAc/hexanes = 1:9) to give the product **6z** (56 mg, 74% yield) as a white solid. ¹H NMR (400 MHz, CDCl₃, 24 °C, δ): 6.72 (d, *J* = 8.3 Hz, 1H), 6.39 (d, *J* = 10.6 Hz, 1H), 6.33 (d, *J* = 8.6 Hz, 1H), 4.24–4.20 (m, 4H); ¹³C{¹H} NMR (100 MHz, CDCl₃, 24 °C, δ): 150.1, 143.8, 137.6, 117.6, 108.5, 104.4, 64.7, 64.2; HRMS (EI) *m/z*: [M]⁺ C₈H₈O₃ calcd for 152.0473; found, 152.0473; FTIR (neat, cm⁻¹): 3436, 1612, 1508, 1313, 1202, 1158, 1067, 912, 759.

3,4-(Methylenedioxypheol 6aa. Using the general procedure, the crude mixture was purified by column chromatography (EtOAc/hexanes = 1:9) to give the product **6aa** (30 mg, 43% yield) as an orange solid. ¹H NMR (400 MHz, CDCl₃, 24 °C, δ): 6.65 (d, *J* = 8.3 Hz, 1H), 6.43 (d, *J* = 2.4 Hz, 1H), 6.25 (dd, *J* = 2.4, 2.5 Hz 1H), 5.91 (s, 2H); ¹³C{¹H} NMR (100 MHz, CDCl₃, 24 °C, δ): 150.7, 148.4, 141.6, 108.3, 106.8, 101.3, 96.4; HRMS (EI) *m/z*: [M]⁺ calcd for C₇H₆O₃, 138.0317; found, 138.0313; FTIR (neat, cm⁻¹): 3410, 2911, 1653, 1633, 1475, 1189, 1135, 1096, 1040, 934.

1-Methyl-1*H*-indol-5-ol 6ab. Using the general procedure, the crude mixture was purified by column chromatography (EtOAc/hexanes = 1:5) to give the product **6ab** (52 mg, 71% yield) as a red solid. ¹H NMR (400 MHz, CDCl₃, 22 °C, δ): 7.19 (d, *J* = 8.7 Hz, 1H), 7.03 (t, *J* = 4.5 Hz, 1H), 6.80 (d, *J* = 8.7 Hz, 1H), 6.35 (br, 1H), 3.76 (s, 3H); ¹³C{¹H} NMR (100 MHz, CDCl₃, 25 °C, δ): 129.8, 111.5, 111.3, 109.9, 105.3, 100.1, 33.1. HRMS (EI) *m/z*: [M]⁺ calcd for C₉H₉NO, 147.0684; found, 147.0684. FTIR (neat, cm⁻¹): 3316, 1523, 1482, 883, 791, 733.

Estrone 6ac. To a solution of estrone-3-boronic acid pinacol ester (**5ac**, 152 mg, 0.4 mmol) and Rh₂(bpy)₂(OAc)₄ (**1**, 6 mg, 0.008 mmol) in anhydrous DMF (40 mL) in a flame-dried flask was added diisopropylethylamine (140 μ L, 0.8 mmol). The reaction mixture was stirred under an atmosphere of oxygen (1 atm) and visible light irradiation (10.5 W white LEDs). After complete consumption of the starting material (24 h, monitored by TLC), the reaction mixture was poured into ice-cold HCl_(aq) (1%, 40 mL) and extracted with EtOAc (5 \times 40 mL). The combined organic extracts were washed with water (2 \times 60 mL) and brine (60 mL), dried over MgSO₄, and filtered. After removal of the solvent under vacuum, the crude product was purified by column chromatography (EtOAc/hexanes = 1:4; dry-loaded) to give **6ac** (68 mg, 63% yield) as a white solid. ¹H NMR (400 MHz, DMSO-*d*₆, 21 °C, δ): 9.03 (s, 1H), 7.03 (d, *J* = 8.4 Hz, 1H), 6.51 (d, *J* = 8.4 Hz, 1H), 6.45 (s, 1H), 2.85–2.64 (m, 2H), 2.41 (dd, *J* = 18.8, 8.4 Hz, 1H), 2.35–2.22 (m, 1H), 2.18–1.83 (m, 4H), 1.80–1.66 (m, 1H), 1.61–1.12 (m, 6H), 0.80 (s, 3H); ¹³C{¹H} NMR (100 MHz, DMSO-*d*₆, 21 °C, δ): 219.7 (C), 155.1 (C), 137.1 (C), 129.9 (C), 126.1 (CH), 115.0 (CH), 112.8 (CH), 49.6 (CH), 47.4 (C), 43.5 (CH), 38.0 (CH), 35.4 (CH₂), 31.4 (CH₂), 29.1 (CH₂), 26.2 (CH₂), 25.6 (CH₂), 21.2 (CH₂), 13.5 (CH₃); HRMS (EI) *m/z*: [M]⁺ calcd for C₁₈H₂₂O₂, 270.1620; found, 270.1612; FTIR (neat, cm⁻¹): 3292, 2936, 2859, 1720, 1620, 1579, 1497, 1454, 1355, 1288, 1248, 1055, 817.

Fluoren-9-one 9. To a solution of fluorene (**10**, 83 mg, 0.5 mmol) and Rh₂(bpy)₂(OAc)₄ (**1**, 8 mg, 0.01 mmol) in anhydrous DMF (50 mL) in a flame-dried flask was added diisopropylethylamine (170 μ L, 1 mmol). The reaction mixture was stirred under an atmosphere of oxygen (1 atm) and visible light irradiation (10.5 W white LEDs). After complete consumption of the starting material (48 h, monitored by TLC), the reaction mixture was poured into ice-cold HCl_(aq) (1%, 50 mL) and extracted with diethyl ether (5 \times 50 mL).

The combined organic extracts were washed with water (80 mL) and brine (80 mL), dried over MgSO₄, and filtered. After removal of the solvent under vacuum, the crude product was purified by column chromatography (EtOAc/hexanes = 1:5) to give **11** (75 mg, 83% yield) as a yellow solid. ¹H NMR (400 MHz, CDCl₃, 24 °C, δ): 7.62 (d, *J* = 8.0 Hz, 2H), 7.53–7.47 (m, 4H), 7.29 (t, *J* = 7.3 Hz, 2H); ¹³C{¹H} NMR (100 MHz, CDCl₃, 24 °C, δ): 194.1, 144.6, 134.8, 134.3, 129.2, 124.5, 120.4; HRMS (EI) *m/z*: [M]⁺ calcd for C₁₃H₈O₂, 180.0575; found, 180.0574; FTIR (neat, cm⁻¹): 3050, 1710, 1605, 1600, 1475, 1377, 1298, 1013, 720.

5-(Iodomethyl)dihydro-2(3*H*)-furanone 11. To a solution of KI (183 mg, 1.1 mmol) and AcOH (380 mg, 5 mmol) in CH₃CN (50 mL) in a flame-dried flask were added pent-4-enoic acid (**12**, 100 mg, 1 mmol) and Rh₂(bpy)₂(OAc)₄ (**1**, 16 mg, 0.02 mmol). The reaction mixture was stirred under an atmosphere of oxygen (1 atm) and visible light irradiation (10.5 W white LEDs). After complete consumption of the starting material (48 h, monitored by TLC), sat. Na₂S₂O₃(aq) (10 mL) was added and the mixture was extracted with EtOAc (3 \times 10 mL). The combined organic extracts were washed with brine (20 mL), dried over MgSO₄, and filtered. After removal of the solvent under vacuum, the crude product was purified by column chromatography (EtOAc/hexanes = 1:10) to give **13** (153 mg, 68% yield) as a yellow oil. ¹H NMR (400 MHz, CDCl₃, 24 °C, δ): 4.58–4.52 (m, 1H), 3.42 (dd, *J* = 10.5, 4.24 Hz, 1H), 3.30 (dd, *J* = 10.5, 4.24 Hz, 1H), 2.70–2.55 (m, 2H), 2.54–2.44 (m, 1H), 2.05–1.95 (m, 1H); ¹³C{¹H} NMR (100 MHz, CDCl₃, 24 °C, δ): 176.3, 78.5, 28.9, 28.2, 7.4; HRMS (EI) *m/z*: [M]⁺ calcd for C₅H₇O₂I, 225.9491; found, 225.9487; FTIR (neat, cm⁻¹): 2954, 1761, 1456, 1415, 1335, 1208, 1151, 1011, 979, 906, 873, 609.

4-Bromo-2-methoxyphenol 13. To a solution of 2-methoxyphenol (55.4 μ L, 0.5 mmol) in anhydrous DMF (50 mL) in a flame-dried flask was added Rh₂(bpy)₂(OAc)₄ (**1**, 20 mg, 0.025 mmol) and CBr₄ (332 mg, 1.0 mmol). The reaction mixture was stirred under an atmosphere of oxygen (1 atm) and visible light irradiation (10.5 W white LEDs). After complete consumption of the starting material (48 h, monitored by TLC), H₂O (50 mL) was added and the mixture was extracted with EtOAc (3 \times 10 mL). The combined organic extracts were washed with brine (80 mL), dried over MgSO₄, and filtered. After removal of the solvent under vacuum, the crude product was purified by column chromatography (EtOAc/hexanes = 1:5) to give **15** (77 mg, 76% yield) as a white solid. ¹H NMR (400 MHz, CDCl₃, 24 °C, δ): 6.98 (d, *J* = 10.5 Hz, 2H), 6.79 (d, *J* = 8.3 Hz, 1H), 5.56 (s, 1H), 3.87 (s, 3H); ¹³C{¹H} NMR (100 MHz, CDCl₃, 24 °C, δ): 147.7, 142.6, 127.0, 113.6, 111.8, 108.8, 56.7; HRMS (EI) *m/z*: [M]⁺ calcd for C₇H₇BrO₂, 201.9629; found, 201.9630; FTIR (neat, cm⁻¹): 3521, 2967, 2946, 2842, 1608, 1505, 1445, 1360, 1258, 1224, 1118, 1026, 859, 839, 810, 781.

ASSOCIATED CONTENT

Supporting Information

The Supporting Information is available free of charge at <https://pubs.acs.org/doi/10.1021/acs.joc.9b02777>.

Visible light photoreaction setup and reaction optimization, spectroscopic data, and details of DFT calculations (PDF)

Crystallographic data for **1** (CIF)

AUTHOR INFORMATION

Corresponding Authors

Michael G. Campbell – Barnard College, New York, New York;  orcid.org/0000-0002-4174-0174; Email: mcampbel@barnard.edu

Gary Jing Chuang – Chung Yuan Christian University, Chung Li, Taiwan;  orcid.org/0000-0001-6058-9185; Email: gjchuang@cycu.edu.tw

Other Authors

Hsiang-Ming Yang – Chung Yuan Christian University, Chung Li, Taiwan
Ming-Lun Liu – Chung Yuan Christian University, Chung Li, Taiwan
Jing-Wen Tu – Chung Yuan Christian University, Chung Li, Taiwan
Emily Miura-Stempel – Barnard College, New York, New York

Complete contact information is available at:
<https://pubs.acs.org/10.1021/acs.joc.9b02777>

Notes

The authors declare no competing financial interest.

ACKNOWLEDGMENTS

We thank Christian Rojas for helpful comments during manuscript preparation. M.G.C. gratefully acknowledges the NSF (CHE-1827936) for an MRI award in support of a 400 MHz NMR spectrometer at Barnard College. E.M.-S. and M.G.C. thank the Department of Chemistry and the Office of the Provost at Barnard for additional financial Support. G.J.C. gratefully acknowledges the Ministry of Science and Technology (MOST) of Taiwan for financial support (108-2113-M-033-007). SCXRD was performed at the Shared Materials Characterization Laboratory at Columbia University.

REFERENCES

(1) (a) Reckenthaler, M.; Griesbeck, A. G. Photoredox Catalysis for Organic Syntheses. *Adv. Synth. Catal.* **2013**, *355*, 2727–2744. (b) Xi, Y.; Yi, H.; Lei, A. Synthetic applications of photoredox catalysis with visible light. *Org. Biomol. Chem.* **2013**, *11*, 2387–2403. (c) Xuan, J.; Xiao, W.-J. Visible-Light Photoredox Catalysis. *Angew. Chem., Int. Ed.* **2012**, *51*, 6828–6838. (d) Narayanan, J. M. R.; Stephenson, C. R. J. Visible Light Photoredox Catalysis: Applications in Organic Synthesis. *Chem. Soc. Rev.* **2011**, *40*, 102–113.

(2) (a) Romero, N. A.; Nicewicz, D. A. Organic Photoredox Catalysis. *Chem. Rev.* **2016**, *116*, 10075–10166. (b) Ravelli, D.; Fagnoni, M.; Albini, A. Photoorganocatalysis. What for? *Chem. Soc. Rev.* **2013**, *42*, 97–113.

(3) (a) Prier, C. K.; Rankic, D. A.; MacMillan, D. W. C. Visible Light Photoredox Catalysis with Transition Metal Complexes: Applications in Organic Synthesis. *Chem. Rev.* **2013**, *113*, 5322–5363. (b) Tucker, J. W.; Stephenson, C. R. J. Shining Light on Photoredox Catalysis: Theory and Synthetic Applications. *J. Org. Chem.* **2012**, *77*, 1617–1622. (c) Shaw, M. H.; Twilton, J.; MacMillan, D. W. C. Photoredox Catalysis in Organic Chemistry. *J. Org. Chem.* **2016**, *81*, 6898–6926.

(4) For a selection of recent reports of photoredox catalysis using molecular oxygen as an oxidant, see: (a) Ariyarathna, J. P.; Wu, F.; Colombo, S. K.; Hillary, C. M.; Li, W. Aerobic Catalytic Features in Photoredox- and Copper-Catalyzed Iodolactonization Reaction. *Org. Lett.* **2018**, *20*, 6462–6466. (b) Wang, H.; Man, Y.; Wang, K.; Wan, X.; Tong, L.; Li, N.; Tang, B. Hydrogen bond directed aerobic oxidation of amines via photoredox catalysis. *Chem. Commun.* **2018**, *54*, 10989–10992. (c) Wu, C.-K.; Liou, T.-J.; Wei, H.-Y.; Tsai, P.-S.; Yang, D.-Y. Visible light photoredox catalysis: aerobic oxidation of perimidines to perimidinones. *Tetrahedron* **2014**, *70*, 8219–8225. (d) Tyson, E. L.; Ament, M. S.; Yoon, T. P. Transition Metal Photoredox Catalysis of Radical Thiol-Ene Reactions. *J. Org. Chem.* **2013**, *78*, 2046–2050. (e) Rueping, M.; Vila, C.; Szadkowska, A.; Koenigs, R. M.; Fronert, J. Photoredox Catalysis as an Efficient Tool for the Aerobic Oxidation of Amines and Alcohols: Bioinspired Demethylations and Condensations. *ACS Catal.* **2012**, *2*, 2810–2815.

(5) Fabry, D. C.; Rueping, M. Merging Visible Light Photoredox Catalysis with Metal Catalyzed C–H Activations: On the Role of Oxygen and Superoxide Ions as Oxidants. *Acc. Chem. Res.* **2016**, *49*, 1969–1979.

(6) For reviews covering dirhodium catalysis in nitrene insertion reactions, see: (a) Roizen, J. L.; Harvey, M. E.; Du Bois, J. Metal-Catalyzed Nitrogen-Atom Transfer Methods for the Oxidation of Aliphatic C–H Bonds. *Acc. Chem. Res.* **2012**, *45*, 911–922. (b) Buendia, J.; Grelier, G.; Dauban, P. Dirhodium(II)-Catalyzed C(sp³)–H Amination Using Iodine(III) Oxidants. *Adv. Organomet. Chem.* **2015**, *64*, 77–118. (c) Darses, B.; Rodrigues, R.; Neuville, L.; Mazurais, M.; Dauban, P. Transition metal-catalyzed iodine(III)-mediated nitrene transfer reactions: efficient tools for challenging syntheses. *Chem. Commun.* **2017**, *53*, 493–508.

(7) For reviews covering dirhodium catalysis in carbene transfer reactions, see: (a) Doyle, M. P.; Duffy, R.; Ratnikov, M.; Zhou, L. Catalytic Carbene Insertion into C–H Bonds. *Chem. Rev.* **2010**, *110*, 704–724. (b) Davies, H. M. L.; Antoulakis, E. G. Recent progress in asymmetric intermolecular C–H activation by rhodium carbenoid intermediates. *J. Organomet. Chem.* **2001**, *617*–618, 47–55.

(8) (a) Whittemore, T. J.; Sayre, H. J.; Xue, C.; White, T. A.; Gallucci, J. C.; Turro, C. New Rh₂(II,II) Complexes for Solar Energy Applications: Panchromatic Absorption and Excited-State Reactivity. *J. Am. Chem. Soc.* **2017**, *139*, 14724–14732. (b) Whittemore, T. J.; Millet, A.; Sayre, H. J.; Xue, C.; Dolinar, B. S.; White, E. G.; Dunbar, K. R.; Turro, C. Tunable Rh₂(II,II) Light Absorbers as Excited-State Electron Donors and Acceptors Accessible with Red/Near-Infrared Irradiation. *J. Am. Chem. Soc.* **2018**, *140*, 5161–5170. (c) Sayre, H. J.; Millet, A.; Dunbar, K. R.; Turro, C. Photocatalytic H₂ production by dirhodium(II,II) photosensitizers with red light. *Chem. Commun.* **2018**, *54*, 8332–8334.

(9) (a) Zou, Y.-Q.; Chen, J.-R.; Liu, X.-P.; Lu, L.-Q.; Davis, R. L.; Jorgensen, K. A.; Xiao, W.-J. Highly Efficient Aerobic Oxidative Hydroxylation of Arylboronic Acids: Photoredox Catalysis Using Visible Light. *Angew. Chem., Int. Ed.* **2012**, *51*, 784–788. (b) Pitre, S. P.; McTiernan, C. D.; Ismaili, H.; Scaiano, J. C. Mechanistic Insights and Kinetic Analysis for the Oxidative Hydroxylation of Arylboronic Acids by Visible Light Photoredox Catalysis: A Metal-Free Alternative. *J. Am. Chem. Soc.* **2013**, *135*, 13286–13289.

(10) Thompson, D. W.; Ito, A.; Meyer, T. J. [Ru(bpy)₃]^{2+*} and other remarkable metal-to-ligand charge transfer (MLCT) excited states. *Pure Appl. Chem.* **2013**, *85*, 1257–1305.

(11) Crawford, C. A.; Matonic, J. H.; Huffman, J. C.; Folting, K.; Dunbar, K. R.; Christou, G. Reaction of Nitrogen Chelates with the [Rh₂]⁴⁺ Core: Bis-Chelate Products and Demonstration of Reversible, Chelate-Based Reduction Processes. *Inorg. Chem.* **1997**, *36*, 2361–2371.

(12) Espino, C. G.; Fiori, K. W.; Kim, M.; Du Bois, J. Expanding the Scope of C–H Amination through Catalyst Design. *J. Am. Chem. Soc.* **2004**, *126*, 15378–15379.

(13) For examples of light on/off experiments in photoredox reactions, see: (a) Theunissen, C.; Ashley, M. A.; Rovis, T. Visible-Light-Controlled Ruthenium-Catalyzed Olefin Metathesis. *J. Am. Chem. Soc.* **2019**, *141*, 6791–6796. (b) Ruhl, K. E.; Rovis, T. Visible Light-Gated Cobalt Catalysis for a Spatially and Temporally Resolved [2+2+2] Cycloaddition. *J. Am. Chem. Soc.* **2016**, *138*, 15527–15530.

(14) Cismesia, M. A.; Yoon, T. P. Characterizing chain processes in visible light photoredox catalysis. *Chem. Sci.* **2015**, *6*, 5426–5434.

(15) (a) Chifotides, H. T.; Dunbar, K. R. Rhodium Compounds. In *Multiple Bonds Between Metal Atoms*; 3rd ed.; Cotton, F. A.; Murillo, C. A.; Walton, R. A., Eds.; Springer: Boston, MA, 2005; pp 465–589. (b) Bursten, B. E.; Cotton, F. A. Electronic Structure of Phosphine Adducts of Tetrakis (carboxylato)dirhodium(II). Pronounced Influence of Axial Ligands. *Inorg. Chem.* **1981**, *20*, 3042–3048. (c) Nichols, J. M.; Wolf, J.; Zavalij, P.; Varughese, B.; Doyle, M. P. Bis(phenyl)-dirhodium(III) Caprolactamate: A Dinuclear Paddlewheel Complex with No Metal–Metal Bond. *J. Am. Chem. Soc.* **2007**, *129*, 3504–3505. (d) Wolf, J.; Poli, R.; Xie, J.-H.; Nichols, J.; Xi, B.; Zavalij, P.; Doyle, M. P. Removal of Metal–Metal Bonding in a Dimetallic Paddlewheel Complex: Molecular and Electronic Structure of

Bis(phenyl) Dirhodium(III) Carboxamide Compounds. *Organometallics* **2008**, *27*, 5836–5845.

(16) Balzani, V.; Bolletta, F.; Gandolfi, M. T.; Maestri, M. Bimolecular electron transfer reactions of the excited states of transition metal complexes. *Top. Curr. Chem.* **1978**, *75*, 1–64.

(17) Arbogast, J. W.; Foote, C. S.; Kao, M. Electron Transfer to Triplet fullerene C₆₀. *J. Am. Chem. Soc.* **1992**, *114*, 2277–2279.

(18) (a) Li, B.; Bi, X.; Zhou, J.; Li, C.; Zhao, P.; Meng, X. Synthesis of Crystalline OMS-2 with Urea Hydrogen Peroxide and its Application in Aerobic Oxidation Reactions. *ChemistrySelect* **2019**, *4*, 6074–6079. (b) Nakai, S.; Uematsu, T.; Ogasawara, Y.; Suzuki, K.; Yamaguchi, K.; Mizuno, N. Aerobic Oxygenation of Alkylarenes over Ultrafine Transition-Metal-Containing Manganese-Based Oxides. *ChemCatChem* **2018**, *10*, 1096–1106.

(19) Ariyarathna, J. P.; Wu, F.; Colombo, S. K.; Hillary, C. M.; Li, W. Aerobic Catalytic Features in Photoredox- and Copper-Catalyzed Iodolactonization Reactions. *Org. Lett.* **2018**, *20*, 6462–6466.

(20) Zhao, Y.; Li, Z.; Yang, C.; Lin, R.; Xia, W. Visible-light photoredox catalysis enabled bromination of phenols and alkenes. *Beilstein J. Org. Chem.* **2014**, *10*, 622–627.

(21) Fulmer, G. R.; Miller, A. J. M.; Sherden, N. H.; Gottlieb, H. E.; Nudelman, A.; Stoltz, B. M.; Bercaw, J. E.; Goldberg, K. I. NMR Chemical Shifts of Trace Impurities: Common Laboratory Solvents, Organics, and Gases in Deuterated Solvents Relevant to the Organometallic Chemist. *Organometallics* **2010**, *29*, 2176.

(22) Li, Z.; Burya, S. J.; Turro, C.; Dunbar, K. R. Photochemistry and DNA photocleavage by a new unsupported dirhodium(II,II) complex. *Phil. Trans. R. Soc., A* **2013**, *371*, 20120128.

(23) Bear, J. L.; Lifsey, R. S.; Chau, L. K.; Ahsan, M. Q.; Korp, J. D.; Chavan, M.; Kadish, K. M. Structural, Spectroscopic, and Electrochemical Characterization of Tetrakis- μ -(2-pyrrolidinonato)-dirhodium(II) and Tetrakis- μ -(δ -valerolactamato)-dirhodium(II). *J. Chem. Soc., Dalton Trans.* **1989**, 93–100.

(24) Doyle, M. P.; Westrum, L. J.; Wolthuis, W. N. E.; See, M. M.; Boone, W. P.; Bagheri, V.; Pearson, M. M. Electronic and Steric Control in Carbon–Hydrogen Insertion Reactions of Diazoacetoacetates Catalyzed by Dirhodium(II) Carboxylates and Carboxamides. *J. Am. Chem. Soc.* **1993**, *115*, 958–964.